Mathematical Analysis of "Phase Ramping" for Super-Resolution Magnetic Resonance Imaging

Gregory S. Mayer and Edward R. Vrscay

Department of Applied Mathematics
Faculty of Mathematics
University of Waterloo
Waterloo, Ontario, Canada N2L 3G1
gsmayer@uwaterloo.ca, ervrscay@uwaterloo.ca

Abstract. Super-resolution image processing algorithms are based on the principle that repeated imaging together with information about the acquisition process may be used to enhance spatial resolution. In the usual implementation, a series of low-resolution images shifted by typically subpixel distances are acquired. The pixels of these low-resolution images are then interleaved and modeled as a blurred image of higher resolution and the same field-of-view. A high-resolution image is then obtained using a standard deconvolution algorithm. Although this approach has been applied in magnetic resonance imaging (MRI), some controversy has surfaced regarding the validity and circumstances under which super-resolution may be applicable. We investigate the factors that limit the applicability of super-resolution MRI.

1 Introduction

Increasing the spatial resolution in magnetic resonance imaging (MRI) has most frequently been performed by optimizing the capabilities of the imaging hardware. However, any improvement in the resolving power of MRI would further increase the efficacy of this versatile modality. Recently, new approaches to resolution enhancement, based on the methodologies of super-resolution (SR) imaging, have been proposed and show promise in increasing the spatial resolution of MRI [5,6,13,19,21].

Super-resolution (SR) image processing is concerned with the enhancement of spatial resolution of images. For example, one may wish to use a number of low resolution images (of various positions and possibly differing resolutions) to produce a higher resolution image of an object. In the classic SR procedure, multiple realizations are collected with a moving field of view (FOV). These multiple images are then used as input to a post-processing reconstruction algorithm that enhances the resolution of the image, overcoming limitations in the system hardware. Readers are referred to the following standard references on the subject [1,3,11,28]. This paper deals with the super-resolution problem in MRI.

A. Campilho and M. Kamel (Eds.): ICIAR 2006, LNCS 4141, pp. 82–93, 2006.

One of the first SRMRI papers [22] that was published was received with controversy. On a qualitative level, results in this article, by Yeshurun and Peled, showed that spatial resolution could be enhanced by acquiring multiple MR images and using a SR technique. However, in [27] it was stated that these results were not reliable. For frequency and phase encoded data, which Yeshurun and Peled implemented (we will describe these encoding methods briefly in the next section), it was noted in [27] that there could be no new information present in each additional image acquired beyond the first image. Therefore, there was no justification for acquiring multiple data sets, and the results obtained in [22] could have been reproduced with a standard interpolation scheme. In response, Yeshurun and Peled agreed with this argument [23]. As a result all subsequent SRMRI papers have avoided using frequency and phase encoded data [5,6,13,19,21]. The purpose of this paper is to revisit the arguments made in [27] and [23] in order to provide a more detailed and mathematical analysis of the basis for super-resolution algorithms when applied to these two encoding schemes, often used in MRI.

There exists an enormous amount of research on resolution enhancement methods in MRI that employ information from only a single acquisition (reviewed extensively in [14,15]). However, we would expect (or hope) that by using more data in an SR approach, more information could be incorporated to increase the image resolution. If this were always true, then SRMRI could have a significant edge over single acquisition techniques. Otherwise, as pointed out in [27], there would be an insufficient justification for the increased scan time needed to acquire more data. It is therefore of great importance to determine any conditions under which additional data sets can yield more information. To the best of our knowledge, this paper represents a first step in this direction. We attempt to analyze mathematically the validity of using multiple acquisitions to enhance spatial resolution in magnetic resonance imaging. In particular, we investigate the possible role of frequency shifting, or "phase ramping," in performing super-resolution MRI. We shall, in fact, show that the amount of independent information that each data set holds is related to the spatial shift applied to the original data.

2 Basic Procedures and Equations in MRI

Let us first briefly outline some typical procedures of acquiring a signal in magnetic resonance imaging. Firstly, MRI data is produced in the form of a continuous analog signal in frequency space. The region of frequency space often takes the form of a rectangular domain, typically centered at the origin and bounded by lines parallel to the coordinate axes.

One of the most common acquisition strategies in MRI is the so-called *2D spin-echo sequence*. In this method, the two image directions in k-space are referred to as the *readout* and *phase encode* directions. The MRI data is usually acquired along a set of trajectories in the readout direction, while assuming a set of discrete values in the phase encode direction. In the readout direction, the signal briefly exists as a continuous entity before it is discretized and used to produce the final image.

The *slice-encoding scheme* is another commonly used technique to spatially encode the measured raw data. SRMRI research has been applied almost exclusively in the slice encoding direction [5,6,13,19,21]. However, in this paper, we shall discuss super-resolution as applied to the method of *frequency encoding*.

For simplicity of notation and presentation, we consider only one-dimensional MRI procedures in this paper. We shall assume that the object of concern is located within the interval $[-R, R]$ on the x-axis. It is the *proton density* of the object, to be denoted as $\rho(x)$ for $x \in [-R, R]$, to which the magnetic resonance spectrometer responds. The fundamental basis of MRI is that different portions of the object, for example, different organs or tissues, possess different proton densities. Visual representations of these differing densities then account for the magnetic resonance "images" of an object.

The (spatially) linearly varying magnetic field in the magnetic resonance spectrometer produces a complex-valued signal $s(k)$ of the real-valued frequency parameter k. The relation between $s(k)$ and the proton density function $\rho(x)$ may be expressed as follows [10,15,9]:

$$s(k) = \int_{-\infty}^{+\infty} \rho(x) \exp(-2\pi i k x) dx. \tag{1}$$

In other words, $s(k)$ is the Fourier transform of $\rho(x)$. If life were ideal, then $\rho(x)$ could be reconstructed from $s(k)$ by simple inverse Fourier transformation. However, there are a number of complications. For example, since the object being imaged has a finite size, its Fourier transform would have to have an infinite support. In practice, however, the frequency response $s(k)$ is obtained for only a finite range of k values. In what follows, we shall assume that the domain over which the signal is measured is a symmetric interval, i.e., $k \in [-k_{max}, k_{max}]$. Following a series of standard post-processing steps to be discussed below, a variety of reconstruction algorithms allow us to estimate $\rho(x)$.

There is also the problem that any practical algorithm must work with discrete data. As such, the analog signal $s(k)$ must be converted into a discrete series. This discretization is accomplished in several steps. Firstly, the signal $s(k)$ must be convolved with an anti-aliasing filter $\psi(k)$ to reduce any aliasing that may occur from sampling. An analog-to-digital converter extracts values of the (frequency) signal at integer multiples of the sampling period, to be denoted as Δk. The entire process may be modelled as follows:

$$L_1(k) = \mathrm{III}\Big(\frac{k}{\Delta k}\Big) \int_{-k_{max}}^{k_{max}} s(\kappa)\psi\big(\frac{1}{K}(k-\kappa)\big) d\kappa, \qquad k \in [-k_{max}, k_{max}], \tag{2}$$

where K represents the (frequency) width of the low-pass filter ψ and $\mathrm{III}(x)$ denotes the so-called *Shah function*, defined as [2]

$$\mathrm{III}(x) = \sum_{n=-\infty}^{\infty} \delta(x-n), \tag{3}$$

where $\delta(x)$ denotes the standard Dirac delta function.

The above integration is performed electronically in a continuous manner on the analog signal. The discrete series $L_1(k)$ represents the filtered and sampled signal that is used in the subsequent digital imaging process. A standard inverse discrete Fourier transform is then applied to $L_1(k)$ to produce a discrete data set $l_1(n\Delta x)$, which is the digital MRI "image" that provides a visual representation of the the proton density function $\rho(x)$ throughout the object.

Finally, we mention that in normal medical imaging applications, e.g., commercial MRI machines, one does not have the luxury of being able to alter the sampling size Δk and anti-aliasing filter $\psi(k)$. This is the assumption that we make in the discussion below.

3 Super-Resolution MRI in the Spatial Domain

Currently, the standard approach to performing super-resolution in MRI is to "fuse" two or more sets of lower resolution spatial data, i.e. magnetic resonance "images" of the proton density function $\rho(x)$, to produce a higher resolution image. In this section, we describe a simple and idealized method of spatial MRI super-resolution.

We assume that two low-resolution, one-dimensional discrete data sets have been acquired from the MRI. For simplicity, we assume that each of these two signals, or "channels", has a uniform sample spacing of Δx and that the sampling of one channel is performed at shifts of Δx from the other. We shall denote these samples as

$$l_1(n\Delta x) \quad \text{and} \quad l_2(n\Delta x + \Delta x/2), \quad n_l = 0, 1, 2, \cdots, N_l - 1. \tag{4}$$

These two channels, which are vectors in $\mathbf{R}^{N_1-1}$, represent *spatially* sampled data. For simplicity, we may consider the discrete l_1 series as a "reference" data set that represents the object being imaged. The second set, l_2, is then obtained by sampling after the object has been shifted by $\Delta x/2$, or one-half the pixel size.

These low-resolution samples are then simply interleaved to produced a merged data set of higher resolution. The discrete merged signal, $m(n\Delta x/2) \in \mathbf{R}^{N_h}$, $n = 0, 1, 2, \cdots, N_h - 1$, where $N_h = 2N_l$, is defined as follows:

$$m(n\Delta x/2) = \begin{cases} l_1(n\Delta x/2) \; n \;\; \text{even} \\ l_2(n\Delta x/2) \; n \;\; \text{odd}. \end{cases} \tag{5}$$

A convolution is then used to model the relationship between $m(n\Delta x)$ and the desired high resolution data set, $h(n\Delta x/2) \in \mathbf{R}^{N_h}$:

$$m(n\Delta x/2) = \sum_{n'=0}^{N_h-1} h(n'\Delta x/2)\phi((n-n')\Delta x/2), \qquad n = 0, 1, 2, \cdots, N_h - 1. \tag{6}$$

The vector $\phi(n\Delta x/2)$ is a point spread function that is estimated using information about the acquisition sequence and/or the object being imaged. After

$\phi(n\Delta x/2)$ has been estimated and $m(n\Delta x)$ has been formed, $h(n\Delta x)$ is found using a chosen deconvolution algorithm.

This is the standard approach adopted for SRMRI [5,6,13,19,21]. However, the "shifted" series l_2 is rarely, if ever, obtained by physically shifting the object being imaged. Normally, the shift is performed "electronically" using the Fourier shift theorem, which will be discussed below.

Finally, the requirement that the two data sets l_1 and l_2 represent one-half pixel shifts can be relaxed to fractional pixel shifts.

4 Super-Resolution MRI in the Frequency Domain

As stated earlier, in order to perform super-resolution, we need at least two data sets that are shifted by fractional pixel lengths. In practice, however, it is difficult to guarantee the accuracy of a spatial shift of the object being imaged (e.g., a patient), especially at subpixel levels. Therefore most, if not all, SRMRI methods simulate the spatial shift by means of the following standard Fourier shift theorem [2]: If $F(k)$ denotes the Fourier transform of a signal $f(x)$, then

$$\mathcal{F}[f(x - \Delta x)] = e^{-i2\pi k\Delta x} F(k). \tag{7}$$

The term $e^{-i2\pi k\Delta x}$ is known as a *linear phase ramp* – the linearity refers to the k variable.

The main problem in magnetic resonance imaging is that one does not work with the raw frequency signal $s(k)$ but rather with a filtered and sampled version of it, namely, the discrete series $L_1(k)$. It is necessary to compare the effects of (i) phase ramping the filtered/sampled $L_1(k)$ series and (ii) phase ramping the raw signal $s(k)$ before filtering/sampling.

– **Case I: Phase ramp applied after filtering/sampling of raw signal** $s(k)$
The process is illustrated schematically below.

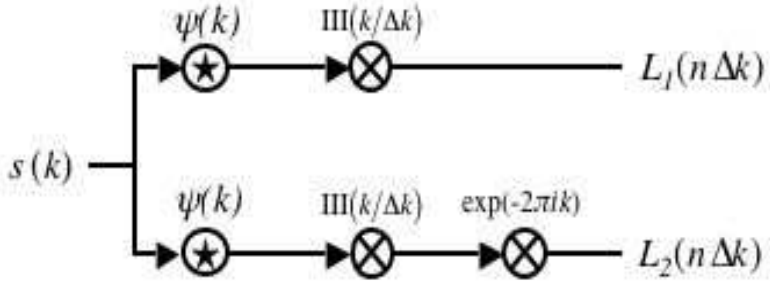

Using Eq. (2), we have the following two series, defined for $k \in [-k_{max}, k_{max}]$,

$$L_1(k) = \mathrm{III}\Big(\frac{k}{\Delta k}\Big) \int_{-k_{max}}^{k_{max}} s(\kappa)\psi(k - \kappa)d\kappa, \tag{8}$$

$$L_2(k) = e^{-i2\pi k\Delta x}\mathrm{III}\Big(\frac{k}{\Delta k}\Big)\int_{-k_{max}}^{k_{max}} s(\kappa)\psi(k-\kappa)d\kappa. \tag{9}$$

Without loss of generality, we have used $K = 1$. Clearly, one can obtain $L_2(k)$ from $L_1(k)$ by multiplying $L_1(k)$ with another phase ramp *after* $\mathrm{III}\Big(\frac{k}{\Delta k}\Big)$ is applied. Therefore, no new information is obtained by constructing $L_2(k)$. This point has been recognized in the literature [23,27].

– **Case II: Phase ramp applied before filtering/samping of raw signal** $s(k)$
The process is illustrated schematically below.

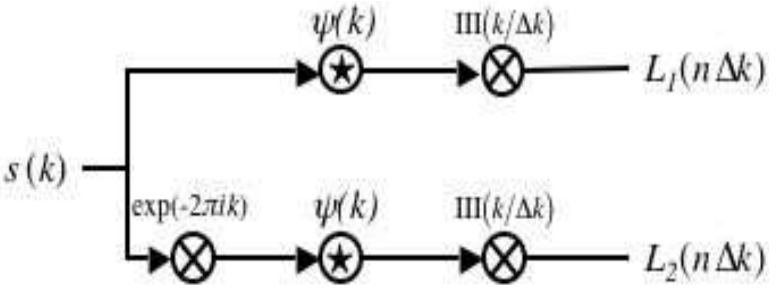

In this case, we have the following two series, defined for $k \in [-k_{max}, k_{max}]$,

$$L_1(k) = \mathrm{III}\Big(\frac{k}{\Delta k}\Big)\int_{-k_{max}}^{k_{max}} s(\kappa)\psi(k-\kappa)d\kappa, \tag{10}$$

$$L_2(k) = \mathrm{III}\Big(\frac{k}{\Delta k}\Big)\int_{-k_{max}}^{k_{max}} s(\kappa)e^{-i2\pi\kappa\Delta x}\psi(k-\kappa)d\kappa \tag{11}$$

Note that the $L_2(k)$ series corresponds to the sampled and filtered data that would be obtained if the object being imaged were physically shifted by $\Delta x/2$ [17].
Unlike Case I, we cannot, in general, obtain $L_2(k)$ from $L_1(k)$ because of the noninvertibility of the operations behind the processing of the signal $s(k)$, namely, convolution and sampling, as well as the "degradation" that is produced by the limited range of integration. These operations are unavoidable in the acquisition process. It would then seem that at least *some* new information is present in $L_2(k)$, which is contrary to what has been claimed in the literature [27]. Unfortunately, it is not clear *how much* more information is added by the second acquisition. This is an open question that we explore in the next section.

Before ending this section, however, we briefly describe how super-resolution MRI can be performed using the L_1 and L_2 series of Case II above. There are at least two avenues:

1. **Performing super-resolution in the spatial domain:** Using the discrete inverse Fourier transform, one can first convert each of the L_1 and L_2 series to the spatial series l_1 and l_2 introduced in Section 2. One then performs super-resolution using the interleaving approach described in that section. In other words, we are performing a standard SR technique to enhance the image quality.
2. **Performing super-resolution in the frequency domain:** In the frequency domain, super-resolution may be accomplished by *frequency extrapolation*, i.e., using low frequency information to estimate high frequency behaviour. There are some standard methods to accomplish such extrapolation, e.g., the Papoulis-Gerchberg algorithm [4,12,20,24,25,26] and projection methods [7,8,14,15,18,29]. We are currently investigating the application of these methods to multiple data sets in the frequency domain, a subject that is beyond the scope of this paper.

4.1 Further Analysis of Case II: Phase Ramping Before Filtering/Sampling

To pursue the question of how much *new* information about $\rho(x)$ is present in the second acquisition, $L_2(k)$ of Case II above, let us generalize our model of the raw MRI data (Eqs. (10) and (11)). We shall consider the spatial shift Δx as a variable parameter which will be denoted as β. The shifted low-resolution signal L_2 is now a function of two variables, i.e.,

$$L_2(k,\beta) = \mathrm{III}\Big(\frac{k}{\Delta k}\Big) I_2(k,\beta), \tag{12}$$

$$I_2(k,\beta) = \int_{-k_{max}}^{k_{max}} s(\kappa) e^{-i2\pi\kappa\beta} \psi(k-\kappa) d\kappa. \tag{13}$$

Clearly, $L_2(k,0) = L_1(k)$. The β-dependence of L_2 lies in the integral I_2.

Assuming that the filter $\psi(k)$ is continuous in k, the integral $I_2(k,\beta)$ is a continuous function of both k and β. However, due to the Shah sampling function, $L_2(k,\beta)$ is nonzero for discrete values of $k \in [-k_{max}, k_{min}]$, which we shall denote as $k_n = n\Delta k$ for appropriate integer values of n, say $-N \le n \le N$, where

$$N = \mathrm{int}\left[\frac{k_{max}}{\Delta k}\right]. \tag{14}$$

Note that the associated sample spacing in the (spatial) image domain is given by

$$\Delta x = \frac{1}{N\Delta k}. \tag{15}$$

In what follows, we shall focus on the amplitudes $I_2(k_n,\beta)$ of the delta function spikes produced by the Shah-function sampling. These amplitudes comprise a $2N+1$-dimensional vector that defines the filtered and sampled signal. For simplicity of notation, we shall denote this vector as $\mathbf{v}(\beta)$, with components

$$v_n(\beta) = I_2(k_n,\beta), \quad n = -N, -N+1, \cdots, N-1, N. \tag{16}$$

The fact that the sampled signal values $v_n(\beta)$ are continuous functions of the spatial shift parameter β does not seem to have been mentioned in the literature. In particular,

$$v_n(\beta) \to v_n(0) = I_1(k_n) \quad \text{as} \ \ \beta \to 0, \tag{17}$$

where

$$I_1(k) = \int_{-k_{max}}^{k_{max}} s(\kappa)\psi(k-\kappa)d\kappa. \tag{18}$$

In fact, it is rather straightforward to show that the function $I_2(k, \beta)$, hence each component of the sampled signal, admits a Taylor series expansion in β which can be generated by formal expansion of the exponential in Eq. (12) followed by termwise integration. (The boundedness of the integration interval $k \in [-k_{max}, k_{max}]$ and the uniform convergence of the Taylor expansion of the exponential over this interval guarantees the convergence of the Taylor expansion for $I_2(k, \beta)$.) The resulting complex-valued series will be written as

$$I_2(k, \beta) = \sum_{m=0}^{\infty} c_m \beta^m \ , \tag{19}$$

where

$$c_m = \frac{(-2i\pi)^m}{m!} \int_{-k_{max}}^{k_{max}} s(\kappa)(\kappa)^m \psi(k-\kappa)d\kappa, \quad m = 0, 1, 2, \cdots. \tag{20}$$

This result would then imply that we could construct the phase ramped signal $v_p(\beta)$ for nonzero values of β from the Taylor series to arbitrary accuracy. But – and this is the important point – we would have to know the coefficients c_m, which means having access to the raw frequency signal $s(k)$, which is not generally possible. In fact, if we had access to $s(k)$, we could compute $L_2(k, \beta)$ directly using Eq.(12)!

We now return to the question of whether additional "information" is being provided by phase ramping. The answer is in the affirmative: Some kind of additional "information" is provided – at least for sufficiently small β values – because the signals $\mathbf{v}(\beta)$ and $\mathbf{v}(0)$ are generally linearly independent for $\beta \neq 0$. (We use the word "generally" because there are exceptional cases, e.g., $s(k) = 0$.) This follows from the definition of the integral $I_2(k, \beta)$ in Eq. (13). It is not generally possible that for a $\beta > 0$, $I_2(k, \beta) = CI_2(k, 0)$ for all values of k (or even k_n).

Unfortunately, at this time we have no method of characterizing this additional "information" in terms of standard information theoretic concepts, e.g., entropy. This implies, of course, that we have no way of quantifying it at present.

As β increases from zero to $\beta = \Delta x/2$, the spatial counterpart of the sampled signal $L_2(k, \beta)$ is shifted from zero pixels to half a pixel. From a spatial resolution viewpoint, with recourse to the equation for L_2 in Case II, we expect that information is added as β increases from zero. Indeed, we are led to conjecture, but cannot prove at present, the following:

Given the two discrete data sets $\mathbf{v}(0)$ and $\mathbf{v}(\beta)$ associated with, respectively, signals $L_1(k)$ and $L_2(k,\beta)$ defined in Eqs. (10), the amount of information added by phase ramping is an increasing function of the shift β over the interval $\beta \in [0, \Delta x/2]$.

In an attempt to study this conjecture, we present a typical result from a series of numerical experiments over a range of β values. In particular, we consider $N = 50$ and $k_{max} = 1$ so that the pixel width is given by $\Delta x = 1/2$. We have chosen

$$s(k) = \mathrm{sinc}^2(10\Delta x k) = \mathrm{sinc}^2(5k), \tag{21}$$

which is the Fourier transform of the triangular proton density function

$$\rho(x) = \begin{cases} \frac{x}{5}, & -5 \le x \le 0, \\ 1 - \frac{x}{5}, & 0 \le x \le 5. \end{cases} \tag{22}$$

The anti-aliasing filter $\psi(k/K)$ is simply a Gaussian function with width $K = \Delta k = 2k_{max}/(2N+1)$. In order to compare $\mathbf{v}(\beta)$ and $\mathbf{v}(0)$, we simply compare the "angle" between the two complex-valued vectors using their complex-valued scalar product,

$$C(\beta) = \cos\theta(\beta) = \frac{\overline{\mathbf{v}}(\beta) \cdot \mathbf{v}(0)}{|\mathbf{v}(\beta)||\mathbf{v}(0)|}, \tag{23}$$

which can be viewed as a kind of "cross correlation" function between the two vectors. In the figure below, we plot numerical values of $C(\beta)$ for $\beta \in [0, 2]$. In all cases, the imaginary parts of $C(\beta)$ are negligible (i.e., zero to at least eight decimal places). At $\beta = 0$, $C(0) = 1$, as expected. As β increases, $C(\beta)$ decreases toward zero, showing that the "angle" between them is increasing toward $\pi/2$.

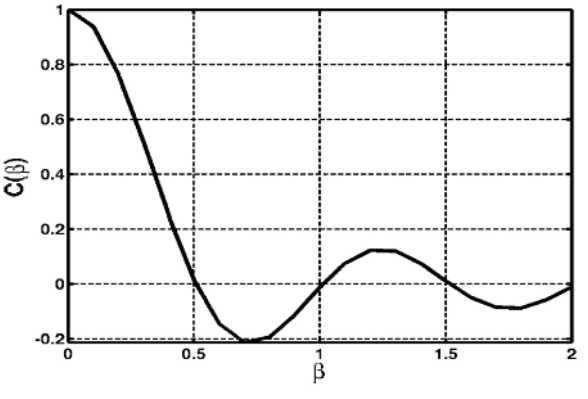

Fig. 1. Plot of angle $\cos\theta(\beta)$, defined in Eq. (23), between vectors $\mathbf{v}(\beta)$ and $\mathbf{v}(0)$ for phase ramping values $0 \le \beta \le 2.0$

5 Discussion and Future Work

In this paper, we have investigated the role of multiple data sets in enhancing the spatial resolution of magnetic resonance imaging, i.e. super-resolution MRI. We agree with the conclusions of [27] and [23] that frequency shifting/phase ramping of postprocessed data does not provide any new information. On the other hand, we have shown that phase ramping of the raw or unprocessed frequency signal $s(k)$ can yield new information, thereby making it possible to perform SRMRI. Of course, it remains to see how much super-resolution can actually be accomplished in the presence of machine noise and other degradation factors. This is the subject of our current work. As well, we are interested in quantifying the additional information provided by phase shifting of the raw frequency signal, so that our conjecture could be stated more rigorously.

Another question concerns the role of the anti-aliasing filter ψ. In the numerical experiments performed to date, a sample of which was presented above, we have used a simple Gaussian filter. It remains to investigate the effects of using other filters as well as their sampling widths. For example, consider the limit in which ψ is a Dirac delta function. Then from Eq. (13), ramping of the frequency signal $v_n = s(k_n)$ produces the signal $v_n = s(k_n)e^{-2\pi i\beta k_n}$ and the cross correlation between signals is given by

$$C(\beta) = \frac{\sum_{n=-N}^{N} s(k_n)^2 e^{-2\pi i\beta k_n}}{\sum_{n=-N}^{N} s(k_n)^2}. \tag{24}$$

We have observed that the values of $C(\beta)$ for this case differ from the experimental results presented in the previous section. Clearly, further analysis is required if we wish to understand and/or quantify the difference.

Acknowledgements

This research was supported in part by the Natural Sciences and Engineering Research Council of Canada (NSERC) in the form of a Discovery Grant (ERV) and a Postgraduate Scholarship (GSM), which are hereby gratefully acknowedged. GSM thanks Prof. J. Ross Mitchell and Dr. Louis Lauzon of the Seaman Family MR Research Center, Foothills Hospital, University of Calgary, Alberta, Canada, for many helpful conversations during his Master's programme. GSM also thanks Dr. Hongmei Zhu, formerly at the Seaman Center and now at York University, Toronto, Ontario, Canada.

References

1. Borman S, Stevenson R, Spatial resolution enhancement of low-resolution image sequences - a review. Proceedings of the 1998 Midwest Symposium on Circuits and Systems, Notre Dame IN, 1998

2. Bracewell R, The Fourier Transform and its Applications. McGraw-Hill, 2nd Edition, 1978
3. Chaudhuri S (Editor), Super-Resolution Imaging. Kluwer Academic Publishers, 2001
4. Gerchberg R W, Super-resolution through Error Energy Reduction. Optica Acta, Vol. 21, No. 9, 709-720, 1974
5. Greenspan H, Peled S, Oz G, Kiryati N, MRI inter-slice reconstruction using super-resolution. Proceedings of MICCAI 2001, Fourth International Conference on Medical Image Computing and Computer-Assisted Intervention (Lecture Notes in Computer Science, Springer, October), 2001
6. Greenspan H, Oz G, Kiryati N, Peled S, MRI inter-slice reconstruction using super-resolution Magnetic Resonance Imaging, 20, 437-446, 2002
7. Haacke M E, Mitchell J, Doohi L, Improved Contrast at 1.5 Tesla Using Half-Fourier Imaging: Application to Spin-Echo and Angiographic Imaging. Magnetic Resonance Imaging, 8, 79-90, 1990
8. Haacke M E, Lindskog E D, Lin W, A Fast, Iterative, Partial-Fourier Technique Capable of Local Phase Recovery. Journal of Magnetic Resonance, 92, 126-145, 1991
9. Haacke M E, Brown R W, Thompson M R, Venkatesan R, Magnetic Resonance Imaging: Physical Principles and Sequence Design. John Wiley & Sons, Inc., USA, 1999
10. Hinshaw W, Lent A, An Introduction to NMR Imaging: From the Bloch Equation to the Imaging Equation. Proceedings of the IEEE, Vol. 71, No. 3, 338-350, 1983
11. Irani M, Peleg S, Motion analysis for image enhancement: resolution, occlusion, and transparency. Journal of Visual Communication and Image Representation, December, 4(4), 324-335, 1993
12. Jain A, Ranganath S, Extrapolation Algorithms for Discrete Signals with Application in Spectral Estimation. IEEE Transactions on Acoustics, Speech, and Signal Processing, ASSP-29, 4, 830-845, 1981
13. Kornprobst P, Peeters R, Nikolova M, Deriche R, Ng M, Hecke P V, A superresolution framework for fMRI sequences and its impact on resulting activation maps. In : Medical Image Computing and Computer-Assisted Intervention-MICCAI 2003, Lecture Notes in Computer Science, 2, Springer-Verlag, 117-125, 2003
14. Liang Z, Boada F E, Constable R T, Haacke M E, Lauterbur P C, Smith M R, Constrained Reconstruction Methods in MR Imaging. Reviews of Magnetic Resonance in Medicine, 4, 67-185, 1992
15. Liang Z, Lauterbur P C, Principles of Magnetic Resonance Imaging, A Signal Processing Perspective. IEEE Press, New York, 2000
16. Margosian P, Schmitt F, Faster MR Imaging: Imaging with Half the Data. Heath Care Instrumentation, 1, 195-197, 1986
17. Mayer G S, Synthetic Aperture MRI. M.Sc. Thesis, The University of Calgary, 2003
18. McGibney G, Smith M R, Nichols S T, Crawley A, Quantitative Evaluation of Several Partial Fourier Reconstruction Algorithms Used in MRI. Magnetic Resonance in Medicine, 30, 51-59, 1993
19. Ng K P, Deriche R, Kornprobst P, Nikolova M, Half-Quadratic Regularization for MRI Image Restoration. IEEE Signal Processing Conference, 585-588 (Publication No. : 76681), 2003
20. Papoulis A, A New Algorithm in Spectral Analysis and Band-Limited Extrapolation. IEEE Transactions on Circuits and Systems, Vol. CAS-22, 9, 735-742, 1975
21. Peeters R, et al, The Use of Super-Resolution Techniques to Reduce Slice Thickness in Functional MRI. International Journal of Imaging Systems and Technology, Vol. 14, 131-138, 2004

22. Peled S, Yeshurun Y, Superresolution in MRI: Application to Human White Matter Fiber Tract Visualization by Diffusion Tensor Imaging. Magnetic Resonance in Medicine, 45, 29-35, 2001
23. Peled S, Yeshurun Y, Superresolution in MRI - Perhaps Sometimes. Magnetic Resonance in Medicine, 48, 409, 2002
24. Sanz J, Huang T, Discrete and Continuous Band-Limited Signal Extrapolation. IEEE Transactions on Acoustics, Speech, and Signal Processing, Vol. ASSP-31, No. 5, 1276-1285, 1983
25. Sanz J, Huang T, Some Aspects of Band-Limited Signal Extrapolation: Models, Discrete Approximations, and Noise. IEEE Transactions on Acoustics, Speech, and Signal Processing, Vol. ASSP-31, No. 6, 1492-1501, 1983
26. Sabri M S, Steenaart W, An Approach to Band-Limited Signal Extrapolation: The Extrapolation Matrix. IEEE Transactions on Circuits and Systems, Vol. CAS-25, No. 2, 1978
27. Scheffler K, Superresolution in MRI? Magnetic Resonance in Medicine, Vol. 48, 408, 2002
28. Tsai R, Huang T, Multiframe image restoration and registration. In: Advances in Computer Vision and Image Processing, JAI Press Inc., 1, 317-339, 1984
29. Youla D, Generalized Image Restoration by the Method of Alternating Orthogonal Projections. IEEE Transactions on Circuits and Systems, Vol. CAS-25, No. 9, 1978